sciendo INTERNATIONAL JOURNAL ON SMART SENSING AND INTELLIGENT SYSTEMS

Research Article | DOI: 10.2478/ijssis-2024-0022 Issue 1 | Vol. 17 (2024)

Machine Learning-based GIS Model for 2D and 3D Vehicular Noise Modelling in a Data-scarce Environment

Biswajeet Pradhan[1,*], Ahmed Abdulkareem Ahmed Aldulaimi[1], Shilpa Gite[2,3], Abdullah Alamri[4] and Subhas Chandra Mukhopadhyay[5]

[1]Center for Advanced Modelling and Geospatial Information Systems (CAMGIS), School of Civil and Environmental Engineering, Faculty of Engineering and Information Technology, University of Technology Sydney, Australia

[2]Computer Science and Information Technology Department, Symbiosis Institute of Technology, Symbiosis International (Deemed) University, Pune 412115, India

[3]Symbiosis Centre of Applied AI (SCAAI), Symbiosis International (Deemed) University, Pune 412115, India

[4]Department of Geology and Geophysics, College of Science, King Saud University, Riyadh, Saudi Arabia

[5]School of Engineering, Macquarie University, NSW 2109 Australia

*E-mail: biswajeet.pradhan@uts.edu.au, biswajeet24@gmail.com

Received for publication June 10, 2024.

Abstract

Vehicular traffic significantly contributes to economic growth but generates frictional noise that impacts urban environments negatively. Road traffic is a primary noise source, causing annoyance and interference. Traditional regression models predict two-dimensional (2D) noise maps, but this study explores the impact and visualization of noise using 2D and three-dimensional (3D) GIS (Geospatial Information Systems) functionalities. Two models were assessed: (i) a 2D noise model for roads and (ii) a 3D noise model for buildings, utilizing limited noise samples. Combining these models produced a comprehensive 3D noise map. Machine learning (ML) models—artificial neural network (ANN), random forest (RF), and support vector machine (SVM)—were evaluated using performance measures: correlation (R), correlation coefficient (R^2), and root mean square error (RMSE). ANN outperformed others, with RF showing better results than SVM. GIS was applied to enhance the visualization of noise maps, reflecting average traffic noise levels during weekday mornings and afternoons in the study area.

Keywords

2D noise model, 3D noise model, artificial neural network, random forest, support vector machine

I. Introduction

Despite the fact that road traffic is inevitable, its annoying sound called noise has continued to draw global attention and possible remedial measures [1–3]. Noise pollution has attracted great interest over the decade [4]. Road traffic is the most widespread source of noise in many countries, and it is the most prevalent cause of annoyance and interference [5–7]. Traffic noise is generated from engine sound and frictional contact between the ground and the vehicle tires [8]. Noise generated from traffic depends on traffic volume, vehicular speed, vehicular class (heavy duty or light cars), and the type of roads [9–13]. Noise prediction is necessary where a future situation cannot be ascertained [14–16]. More so, field measurement of noise pollution seems impractical and difficult

Open Access. Published by Sciendo. CC BY-NC-ND
© 2024 Pradhan et al. This work is licensed under the Creative Commons Attribution-NonCommercial-NoDerivs 4.0 License https://creativecommons.org/licenses/by-nc-nd/4.0/

since numerous points are required to be measured to ascertain the true position of the noise situation [17–20].

So, a considerable amount of work has been carried out with the aim of developing models to predict noise levels generated from road traffic. Urban noise maps have been developed in many countries. Most noise maps were produced in a two-dimensional (2D) format by measuring noise levels on a grid of 10 m horizontally and 4 m above the ground. Although the 2D maps are adequate in low-density urban areas where most buildings have only a few stories [21–28]. The accuracy reduces with an increase in the density of the population especially in urban areas where elevation of most buildings is too high. Three-dimensional (3D) noise maps are required for precise characterization of noise levels in major urban cities surrounded by high-rise buildings [29–35].

However, very little effort has been witnessed in relation to the 3D noise maps predicted in the past with different noise prediction models and tools [31–34]. Therefore, if 3D noise maps are properly generated and predicted, it would enable planners and architects to locate and orientate their buildings appropriately at the design stage. This would ensure improved noise reduction and a serene environment. It would also improve the quality of life and reduce health risks associated with noise that could arise from long-term exposure to excessive noise levels [36, 37]. The 2D GIS (Geospatial Information Systems) has been widely and successfully used in environmental impact studies to assess the impact of spatial phenomena such as soil pollution, air pollution, and noise, on the environment [38–44]. However, it can be expected that the proposed 3D approach can offer fundamental improvements when 3D effects are relevant in urban areas.

There are studies in an effort to produce 3D noise maps, for instance, 3D noise map in Paris was created with the French standard NMPB-Route-96 [45] and the geometric data acquired from digital photographs [33, 45]. 3D noise mapping in Hong Kong was reported recently [46]. It was carried out with customized LimA packages using international standard ISO-9613-2 [47] for territory-wide mapping. The UK standard CRTN [48] was applied for project-based 3D mapping. Also, 3D noise mapping using the Dutch standard SMM1 was presented [30, 49]. These models cannot be imported into commercial software for noise mapping as noise propagation algorithms deployed in the commercial software are basically 2.5-dimensional (2.5D).

However, several studies carried out were mainly focused on the production of either 2D noise maps or 3D maps based on a large number of noise samples. This approach proved to be expensive and time-consuming as it required a number of noise samples to produce 3D noise maps with high accuracy. Therefore, the objective of this research is to produce noise impact and improve visualization by using basic 2D and 3D GIS functionalities and to increase the accuracy of noise impact assessment studies by building two models: 2D noise model for roads and 3D noise model for buildings by using fewer noise samples. The samples (2D and 3D) are then combined to produce 3D noise map for the capital of the study area.

II. Study Area

This study was carried out in the capital city of Kirkuk, Iraq. This study area was chosen for its features such as industrial and residential buildings characterized by low/high-density population which makes it suitable for noise-related investigations. According to the Iraq Ministry of Planning, Kirkuk is the capital of Iraqi culture that is characterized by high traffic flow. It embodied different types of road networks such as Baghdad Erbil (BE) expressway, primary, and secondary roads all located in the city. These diversities make the site suitable for traffic noise studies. Figure 1 shows the study area.

III. Noise Data and Predictor Variables

The dependent variable of the model is noise levels (time-averaged sound pressure level). It is the equivalent steady level over a given period of time that contains the same amount of noise energy as the actual fluctuating level. Measurements of noise were taken at random sites (selected randomly with the use of the ArcGIS Sampling Design Tools) across the city. The measurements were performed using a CESVA SC102 sound level meter (class 2 ± 0.7 dB). The noise level was measured (dB (A)—Decibel A-weighted) at each site every 20-min and 1.5 m above ground. Measurements were taken in the rush hours of morning (7:00–9:00) and afternoon (12:00–2:00) during summer between March 12 and 15, 2018.

Measurements were taken at various locations such as on and near highways and main roads, back streets (side streets with low noise levels), and

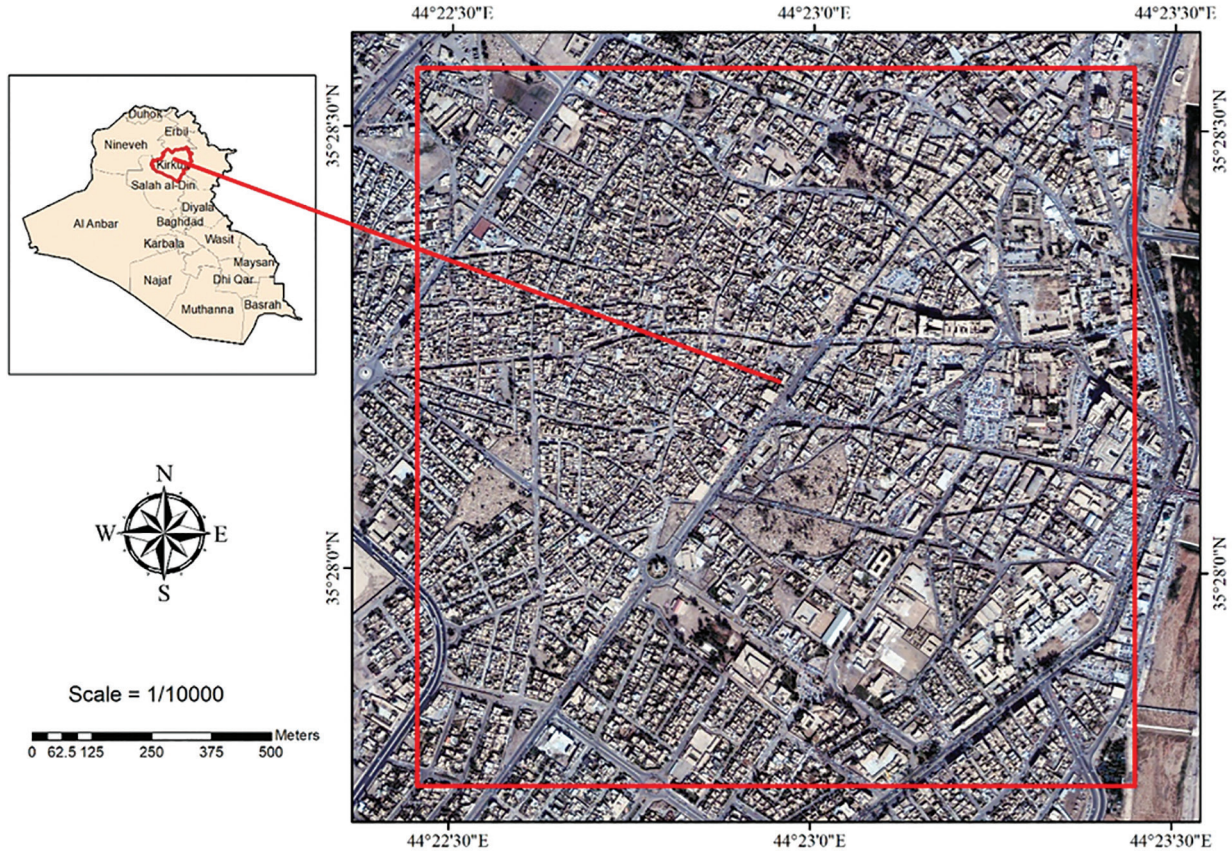


Figure 1: The study area.

different floors of buildings every 20 min during rush hour. Additional data were collected from traffic flows. A total of 26 measurements were performed (Figure 2), where the 26 noise samples for the 3D noise model were split into 18 for training and 8 for testing, and the 9 noise samples for the 2D noise model were split into 6 for training and 3 for testing of the model.

The purpose of this study is to estimate the traffic noise level for a given location. The noise parameters of the model were determined and selected based on an evaluation taking into account the traffic and weather characteristics of the area under consideration. The noise parameters for the 2D noise model are semitrailer, truck, bus, light vehicle, motorbike, digital surface model (DSM), average speed, and maximum speed, whereas for the 3D noise model are the distance from high light vehicle, medium light vehicle, low light vehicle, high truck, medium truck, low truck, high motorbike, medium motorbike, low motorbike, high semitrailer, medium semitrailer, low semitrailer, high bus, medium bus, low bus, medium average speed, low average speed, high maximum speed, medium maximum speed, low maximum speed, high average speed, and DSM.

The parameters of 2D and 3D noise models were summarized based on statistics as shown in Table 1. Figure 3A shows the type of road network parameter; Figure 3B shows low, medium, and high light vehicle parameters; Figure 3C shows low, medium, and high truck parameters; Figure 3D shows low, medium, and high motorbike parameters; Figure 3E shows low, medium, and high semitrailer parameters; Figure 3F shows low, medium, and high bus parameters; Figure 3G shows low, medium, and high of average speed parameter; Figure 3H shows low, medium, and high of maximum speed parameters; Figure 3I shows the DSM for the study area.

IV. Methodology

Figure 4 presents the methodology adopted in the proposed model, which is a combination of 2D and 3D models of traffic noise based on machine learning (ML). The traffic noise prediction maps were produced depending on the GIS model. In this study,

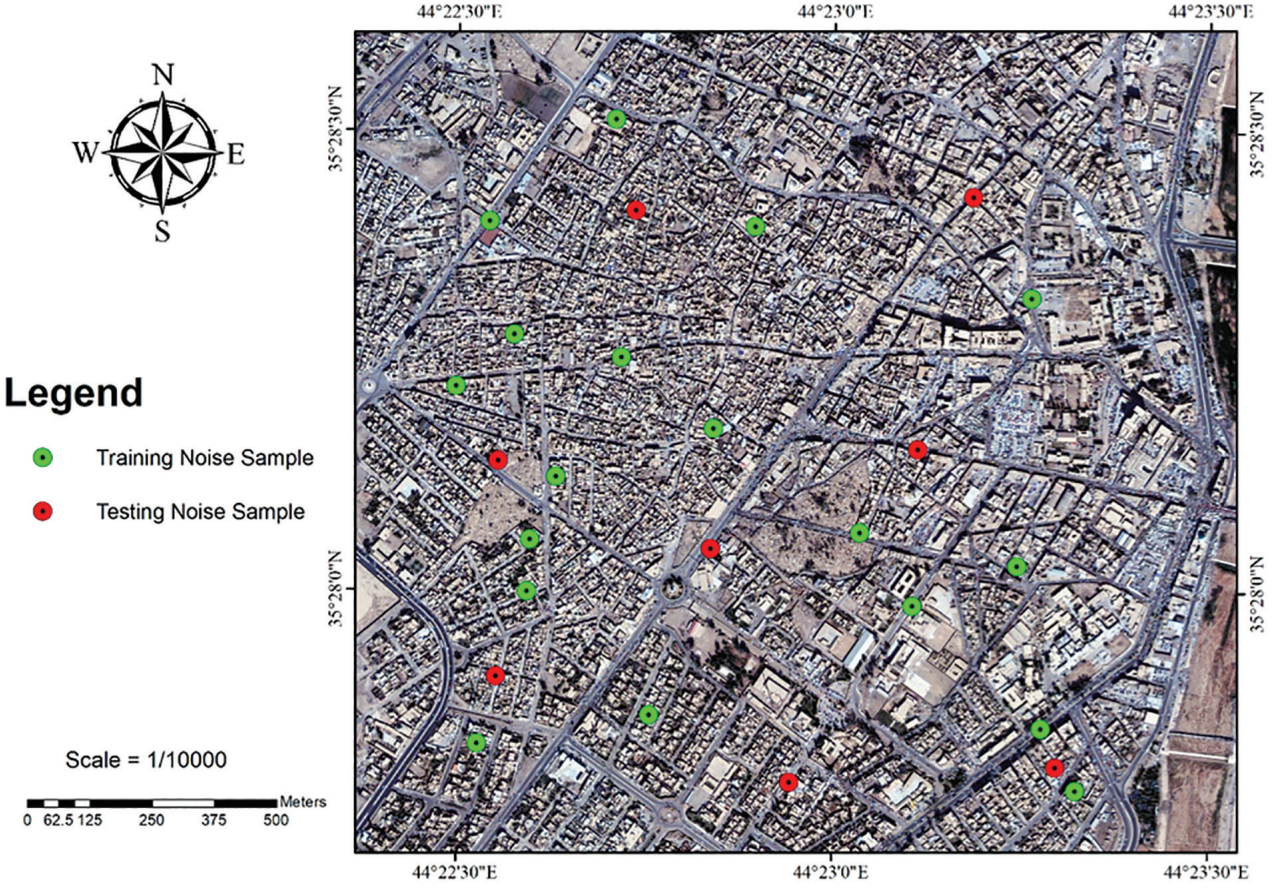


Figure 2: Training and testing noise samples in the study area.

remote sensing data using DSM raster and Quickbird image were used. The data such as traffic volume and traffic noise were collected using a field survey in the city capital, Kirkuk. Data sets were prepared and maintained in a GIS database and predicted traffic noise maps were generated using GIS. The multilevel prediction models were developed using three ML methods such as artificial neural network (ANN), random forests (RFs), and support vector machine (SVM) and the input parameters for the 2D noise model are light vehicle, truck, motorbike, semitrailer, bus, DSM, average speed, and maximum speed.

The input parameters for the 3D noise model are distance from high light vehicle, distance from medium light vehicle, distance from low light vehicle, distance from high truck, distance from medium truck, distance from low truck, distance from high motorbike, distance from medium motorbike, distance from low motorbike, distance from high semitrailer, distance from medium semitrailer, distance from low semitrailer, distance from high bus, distance from medium bus, distance from low bus, distance from high average speed, distance from medium average speed, distance from low average speed, distance from high maximum speed, distance from medium maximum speed, distance from low maximum speed, and DSM.

The location of noise samples and the output or dependent parameter is the equivalent continuous sound pressure level every 20 min ($L_{eq,20}$ dB(A)) during the rush hours of weekday morning and afternoon. Furthermore, the results of the proposed model and other models were validated based on correlation (R), correlation coefficient (R^2), and root mean square error (RMSE) algorithms. Finally, the prediction of 2D and 3D noise maps for the study area based on the best model achieves less RMSE.

a. ML models

In this study, three different ML models such as ANN, RF, and SVM were applied for the 2D and 3D noise models. The best performance among the three

Table 1: Statistical summary of noise predictors of 2D and 3D noise models

Parameter	Minimum	Maximum	Mean	Deviation
Average noise	28.21	83.28	47.71	20.14
Light vehicle	0.00	354.00	20.15	70.01
Truck	0.00	92.00	8.69	22.76
Motorbike	0.00	29.00	2.00	5.87
Semitrailer	0.00	108.00	5.53	21.39
Bus	0.00	129.00	9.69	26.92
DSM	2.47	29.2	13.73	15.66
Average speed	0.00	49.64	11.65	17.02
Maximum speed	0.00	66.00	13.69	21.57
Distance from high volume of light vehicle	0.00	1079.08	432.70	261.98
Distance from medium volume of light vehicle	0.00	1002.72	252.37	239.22
Distance from low volume of light vehicle	0.00	539.36	58.45	103.52
Distance from high volume of truck	0.00	628.94	220.19	164.74
Distance from medium volume of truck	0.00	594.40	119.59	129.21
Distance from low volume of truck	0.00	738.88	120.67	161.98
Distance from high volume of motorbike	0.00	1157.50	468.80	268.63
Distance from medium volume of motorbike	0.00	926.08	243.85	233.62
Distance from low volume of motorbike	0.00	569.75	65.09	114.28
Distance from high volume of semitrailer	0.00	1549.70	636.87	378.83
Distance from medium volume of semitrailer	0.00	849.06	250.78	191.34
Distance from low volume of semitrailer	0.00	379.29	25.43	47.44
Distance from high volume of bus	0.00	910.39	158.78	208.53
Distance from medium volume of bus	0.00	445.29	84.82	88.49
Distance from low volume of bus	0.00	1059.13	295.93	272.59
Distance from high volume of average speed	0.00	666.25	141.29	137.27
Distance from medium volume of average speed	0.00	406.50	78.55	81.38
Distance from low volume of average speed	0.00	652.80	117.52	129.15
Distance from high volume of maximum speed	0.00	722.50	170.70	178.77
Distance from medium volume of maximum speed	0.00	442.07	75.57	84.09
Distance from low volume of maximum speed	0.00	829.62	179.87	195.56

2D, two-dimensional; 3D, three-dimensional; DSM, digital surface model.

models was evaluated using correlation (R), correlation coefficient (R^2), and RMSE to estimate $L_{eq,20\,min}$.

a.i. Neural network architecture model (ANN)

ANN is considered a ML technique, but it uses biological and statistical learning models. ANNs are used to model system states using nonlinear combinations of input variables [50–54]. The ANN used in this work is a backpropagation network with a sigmoidal activation function in the hidden layer and a linear activation function in the output node. According to Bishop [55], our architecture has only one hidden layer because multiple hidden layers are often not explored. The ANN is trained using a backpropagation algorithm with gradient descent and momentum terms.

ANNs are required to specify the learning rate, the number of nodes in a single hidden layer, and the maximum number of training epochs [56]. In this

study, the optimal number error approach was used. The number of hidden layers varied from 3 to 30, and the learning rate varied from 0.01 to 0.8, with increment levels of 0.05. Table 2 shows the hyperparameters of ANN model for traffic noise prediction using the search space. We calculated the RMSE and R^2 between the model output and the measured data for each configuration. The ANN algorithm is based on the principle of error minimization by iterative gradients as in Eq. (1). ANN model uses remote sensing

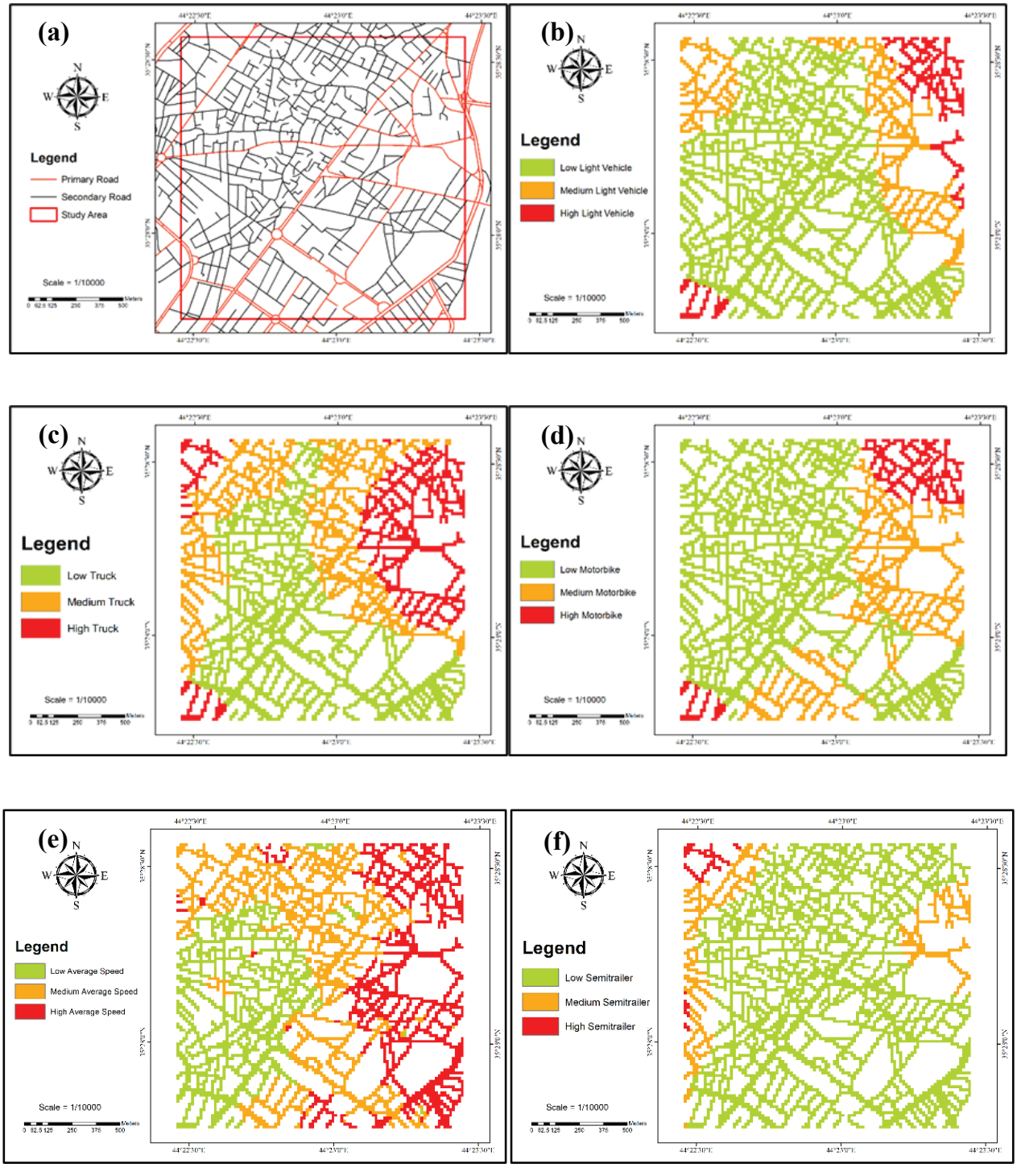


Figure 3: Continued.

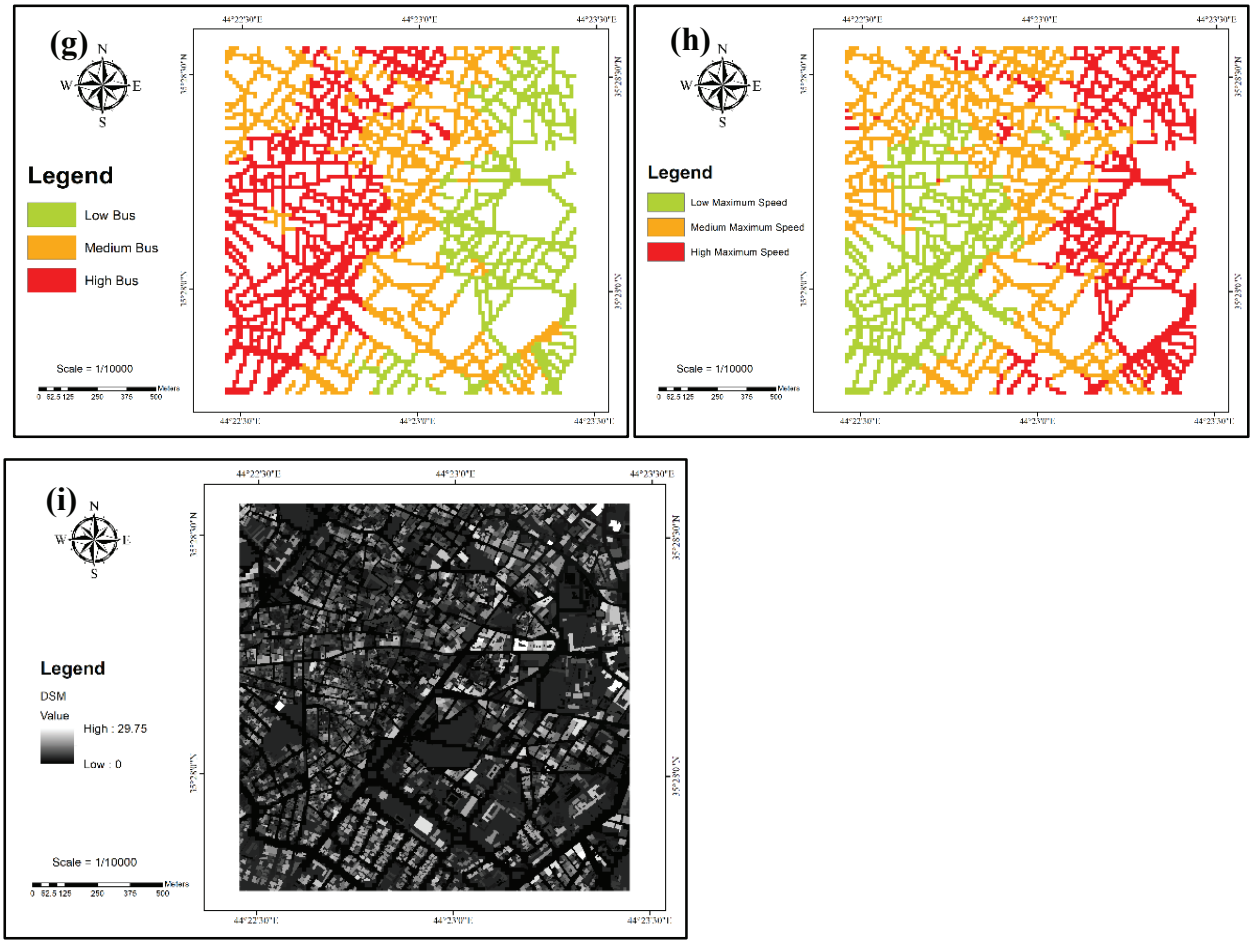


Figure 3: Different spatial data used in this study: (A) Road networks; (B) Low, medium, and high light vehicles; (C) Low, medium, and high trucks; (D) Low, medium, and high motorbike; (E) Low, medium, and high semitrailer; (F) Low, medium, and high bus; (G) Low, medium, and high average speed; (H) Low, medium, and high maximum speed; (I) DSM. DSM, digital surface model.

applications because it has been very successful [57].

$$E = \frac{1}{2}\sum_{i=1}^{L}\left(d_j - o_j^M\right)^2 \quad (1)$$

where d_j and o_j^M represent the desired output and current response of node "j" in the output layer, respectively, and "L" is the number of nodes in the output layer. In the iterative process, the weight parameter correction is calculated and added to the previous value, as shown below:

$$\begin{cases} \Delta w_{i,j} = -\mu\dfrac{\partial E}{\partial w_{i,j}} \\ \Delta w_{i,j}\left(t+1\right) = \Delta w_{i,j} + \alpha\Delta w_{i,j}\left(t\right) \end{cases} \quad (2)$$

where $w_{i,j}$ is the weight parameter between nodes i and j, Δ is a positive constant controlling the amount of adjustment called the learning rate, α is a momentum factor, which can take values between 0 and 1, and "t" denotes the number of iterations. The α parameter smoothes abrupt the rapid changes between weights. It is therefore called the smoothing factor or stabilization factor [58].

a.ii. RF model

The RF algorithm is a supervised classification algorithm [59, 60]. As the name suggests, create a forest and randomize it. There is a direct correlation between the number of trees in the forest and the results that can be produced: the more trees, the

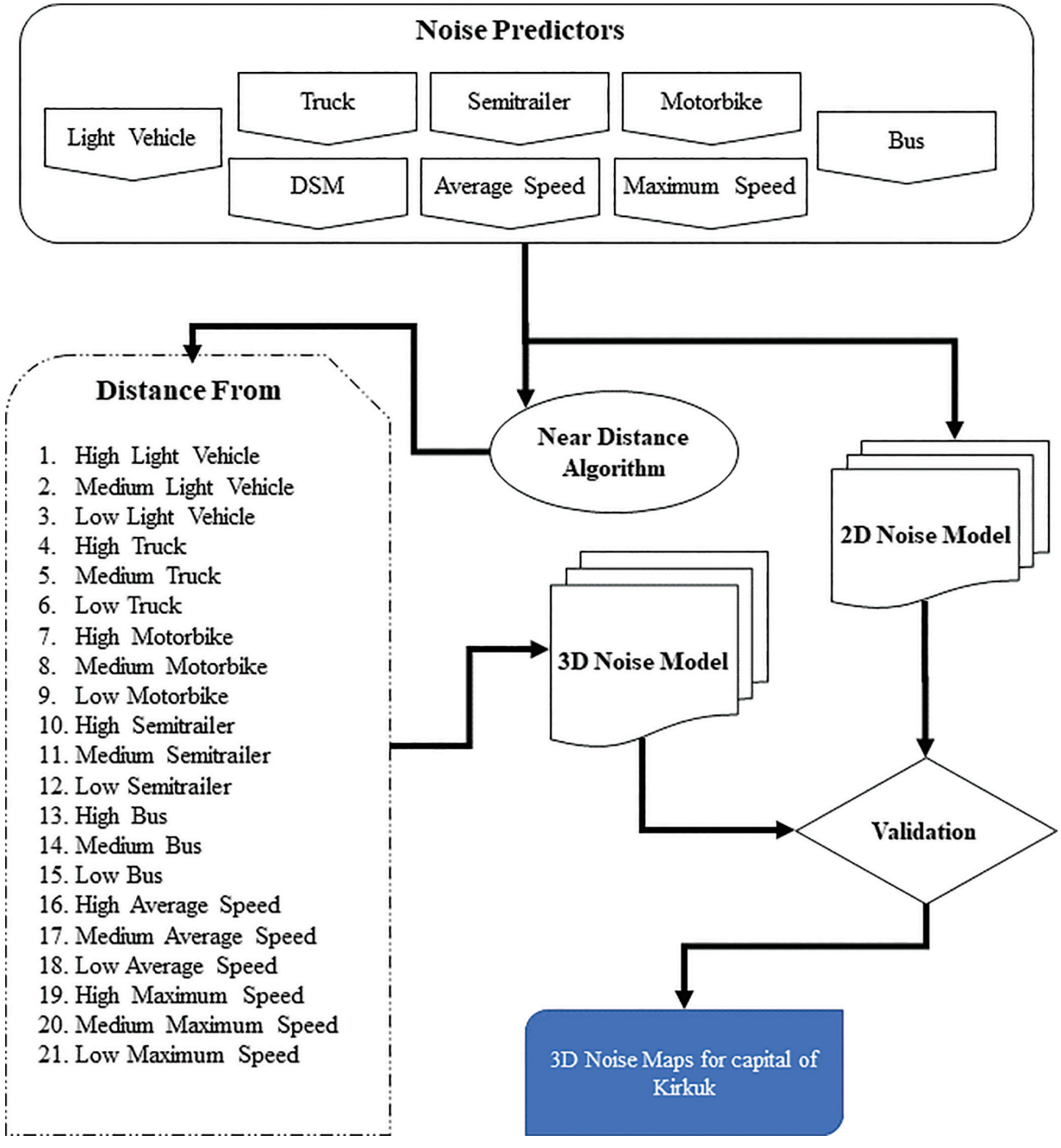


Figure 4: Methodology used in this work.

more accurate the results. However, creating a forest is not the same as creating decisions using an information-gain or gain-index approach. It can be used for both classification and regression tasks. However, overfitting is a serious problem that can invalidate your results. For RF algorithms, the classifier does not overfit the model if there are enough trees in the forest. In addition, RF classifiers can handle missing values and model categorical values [59–62].

The RF algorithm works in two phases. One phase is to create a RF and another phase is to make predictions from the RF classifier created in the first phase [63].

1. Randomly select "K" features from total "m" features where k << m.
2. Among the "K" features, calculate the node "d" using the best-split point.

Table 2: Hyperparameters of the proposed model for traffic noise prediction and their search space used for fine-tuning

Hyperparameters	Search domain
Type of network	{multilayer perceptron (MLP)}
Number of hidden units	(3–30)
Training algorithm	{BFGS, RBFT}
Hidden and output activation	{Identity, Logistic, Tanh, Exponential, Gaussian}
Learning rate	(0.01–0.9) by step of 0.05
Momentum	(0.1–0.9) by step of 0.1

3. Split the node into daughter nodes using the best split.
4. Repeat steps 1–3 until "l" number of nodes has been reached.
5. Build a forest by repeating steps 1–4 for "n" number of times to create "n" number of trees.

In the next stage, with the RF classifier created, prediction can be made. The RF prediction pseudocode is shown below:

1. Take the test features, use the rules of each randomly created decision tree to predict the outcome, and store the predicted outcome (target).
2. Calculate the votes for each predicted target.
3. Consider the high-voted predicted target as the final prediction from the RF algorithm.

a.iii. SVM model

SVR is a ML algorithm used for nonlinear regression that can be used as a universal approximation for multivariate tasks with any level of accuracy [64, 65]. The SVR model is applied to predict the dependent variable "y" depending on the set of independent variables "x," as presented in Eq. (3):

$$y = \left(w^T . \varnothing(X) + b\right) + \text{noise} \tag{3}$$

where the model's noise is represented by the tolerance (ε). w represents a coefficient vector and b represents a constant value. A kernel function, denoted Φ, is used to transform the data values into a higher-dimensional feature space, making them easier to separate than the original space. The task is to find the functional form of w^T. ∅(X) + b. This shape can be obtained by adjusting the model. The reduction of the error function was used to derive w and b from Eqs. (4)–(6):

$$\frac{1}{2} w^T . \text{w} + \text{C}\sum_{i=1}^{N} \varepsilon i + \text{C}\sum_{i=1}^{N} \varepsilon . \text{i} \tag{4}$$

$$w^T . \varnothing(\text{X}) + \text{b} - \text{yi} \le \varepsilon + \varepsilon . \text{i} \tag{5}$$

$$\varepsilon.\text{i}, \varepsilon.\text{i} \ge 0, \text{i} = 1, \ldots\ldots, \text{N} \tag{6}$$

where C specifies a positive constant that determines how much loss is penalized if a calibration error occurs, N is the sample size, ε.i and εi are slack variables that specify the upper and lower calibration errors, respectively, as a function of ε.

b. Noise model

In this study, two models were built for traffic noise: (i) 2D traffic noise and (ii) 3D traffic noise. In each model, the prediction of the traffic noise was based on three methods namely, ANN, RF, and SVM algorithms. These methods are used in Python for predicting $L_{eq,20}$ *min*. These applications in different soft computing approaches are used to find the best noise prediction map of $L_{eq,20}$ for the capital of Kirkuk, Iraq. These methods are evaluated based on correlation (R), correlation coefficient (R^2), and RMSE. Moreover, the correlation and variance inflation factor (VIF) of the model parameters were calculated and validated to get the best model. Finally, after the identification of the best model through validation from training and testing data, the $L_{eq,20}$ maps are produced using GIS techniques for the study area.

b.i. 2D noise models

This model is designed for all types of roads. First, three landuse types (residential, commercial, and industrial) were extracted. These layers have been converted to spatially constrained points so that they are constrained to be generated within the landuse polygon. A search radius of 100 m was then used to estimate the density of the points and the resolution was set to 9 m for the output density grid, and then combined using different weights of 1, 2, and 3 for residential, commercial, and industrial. A composite density grid was created covering the study area. The combined density raster was rescaled from 0 to 1 using a linear method. Inclusion is the generated grid for select noise samples in the study area.

An inclusion probability grid was used to generate spatially balanced points within the study area.

The number of points generated in the study area depends on the total length of the road network. The generated points are distributed within the boundaries of the study area. Therefore, selecting the final noise samples based on transport characteristics requires an additional processing step to adjust the generated points. A size 9 tessellation grid was generated to cover the study area, the grid that intersected the generated points and transport features was selected, and the rest of the tessellation grid was removed. Noise samples were selected within the rest of the mosaicked lattice and transport features. Now, one can predict the traffic noise around a chosen point. The generated road traffic noise is simulated using several models such as ANN, RF, and SVM algorithms. Models are evaluated to select the best predictive model based on correlation (R), correlation coefficient (R^2), and RMSE. The noise parameters input to the model are light cars, trucks, motorcycles, trailers, buses, DSM, average speed, and maximum speed. Finally, a GIS model was spatially designed to represent the predicted traffic noise levels produced by vehicular traffic on highways. The design is based on the final implementation of the proposed model (best model).

The model parameters were converted to a geodatabase by connecting different locations obtained using attributes and GPS. To obtain correct noise prediction information, we used geostatistical interpolation (Inverse distance weighted (IDW) interpolation) to further transform the parameters into stars. The IDW method was chosen because it provides highly correlated results compared to the spline and kriging methods. On the other hand, the spline and kriging results show more distortion in the interpolated results compared to the IDW. A high-resolution 3 × 3 m grid was applied to predict road traffic noise in unsampled regions. Each raster shows the intersection-based values for the difference in traffic noise values and the distribution of the resulting traffic noise levels.

b.ii. 3D noise models

The 3D model of the noise was achieved by dividing the study area into 3 × 3 × 3 m^3 to generate the observation point as 3D and apply a similar procedure as in the 2D model [66]. The 3D building model was prepared based on a DSM raster. The 3D noise model was applied to buildings only. The noise prediction variables in the model were based on GIS data, including road networks, traffic volumes, traffic speeds, land use coverage, and DSMs collected from both public and government data.

So, the spatial noise predictor parameters inputted into the model are: distance from high light vehicle, distance from medium light vehicle, distance from low light vehicle, distance from high truck, distance from medium truck, distance from low truck, distance from high motorbike, distance from medium motorbike, distance from low motorbike, distance from high semitrailer, distance from medium semitrailer, distance from low semitrailer, distance from high bus, distance from medium bus, distance from low bus, distance from high average speed, distance from medium average speed, distance from low average speed, distance from high maximum speed, distance from medium maximum speed, distance from low maximum speed, and DSM. The spatial noise predictors were calculated by using the nearest algorithm available on GIS to calculate the distance from the nearest noise predictors (of any type) to the centroid in the grid in meters. The intersection of the building data with the grid cell is used to calculate the total area of building coverage in each cell and divided by the grid cell area to get the percentage of the building coverage in each grid cell.

The data preparation for use as input in the ML models (ANN, RF, and SVM), the R, R^2, and RMSE for all models were calculated from ML. The best model was chosen depending on the evaluated algorithms. The final model is then linked and integrated into GIS. Finally, the conversion algorithm was used to convert the data to feature and combine it with 2D prediction noise map for subsequent production of 3D noise map.

V. Model Evaluation

The performance of the three models was determined by calculating three performance measures: correlation (R), correlation coefficient (R^2), and RMSE, which can give an estimated Leq value. Four performance measures were used to assess the predictive power of the model. These performance measures measure the accuracy of a model's predictions by comparing the actual parameter values a_i, the predicted values b_i, and the number of sample data points n with, for example, the mean of all observations indicate and the mean of all predicted values (b_i). This can be useful when comparing different models.

First, Eq. (7) shows the correlation between the two data sets to calculate the linear relationship. The

value of R is between –1 and +1. Then, using Eq. (8), the coefficient of determination was calculated and the resulting value for R^2 is between –1 and +1. Finally, the RMSE is calculated using Eq. (9) to assess the average performance of the model across different test samples [66].

$$R = \frac{\sum_{i=1}^{n}\left(a_i - \bar{a}\right)\left(b_i - \bar{b}\right)}{\sqrt{\sum_{i=1}^{n}\left(a_i - \bar{a}\right)^2 \sum_{i=1}^{n}\left(b_i - \bar{b}\right)^2}} \tag{7}$$

$$R^2 = \left(R\right)^2 \tag{8}$$

$$RMSE = \sqrt{\frac{\sum_{i=1}^{n}\left(\left|bi - ai\right|\right)^2}{n}} \tag{9}$$

VI. Results and Discussion

a. Results of ANN

Figures 5A,B shows the proposed network architectures designed for 2D and 3D receptive noise prediction. Here, about 500 networks have been trained with various combinations and parameters. The ANN output model is identified by the average noise level (dB) $L_{eq,20}$. These designs are based on the network structure results and optimized hyperparameters presented in Section 4.1.1. According to the 2D noise prediction results, the model of this study was achieved with 18 hidden layers and 8 input parameters. Also, the best-trained network was with the BFGS algorithm, whereas the best hidden and emitted activation was ID; the optimal gradient pulse and learning rate is 0.3.

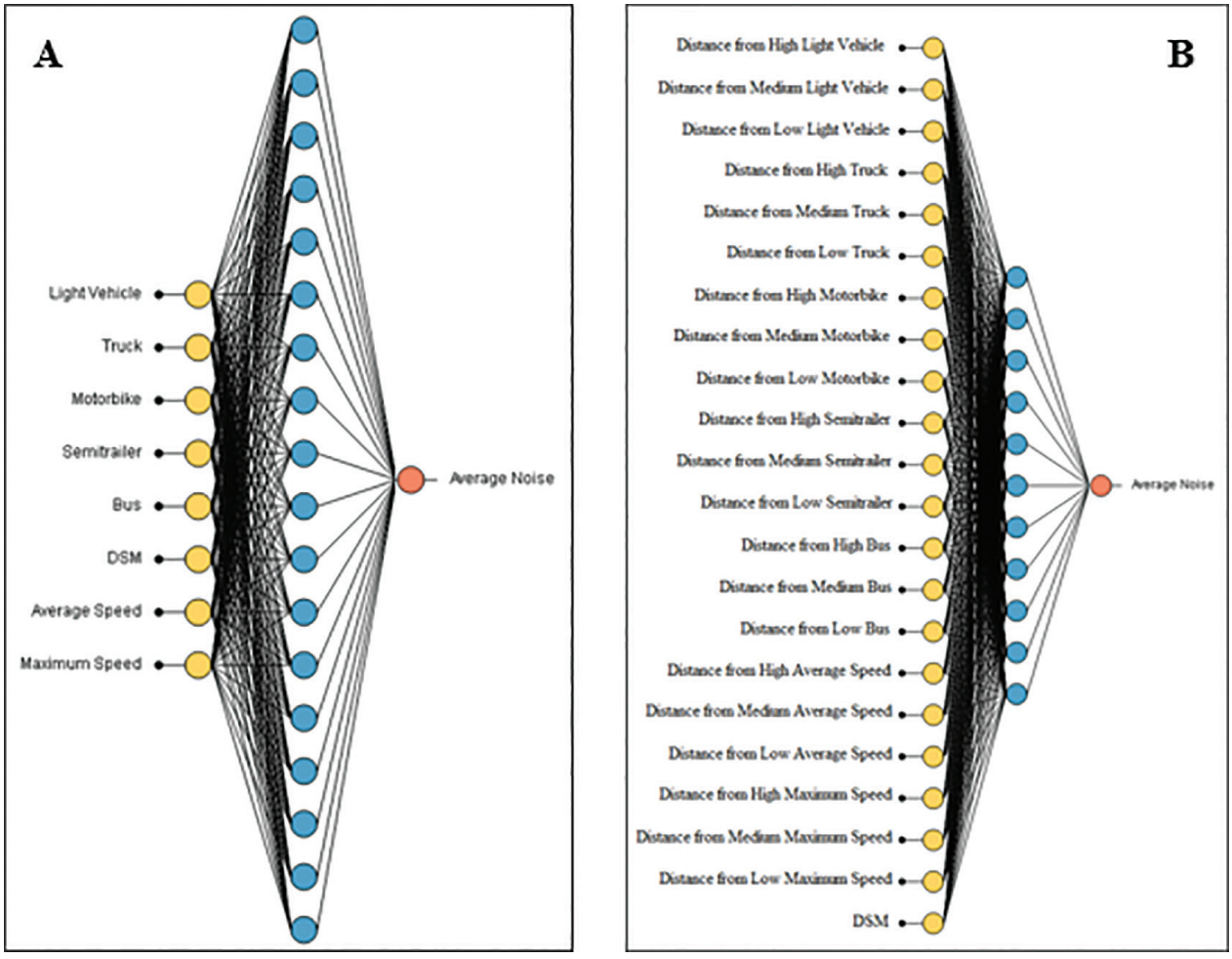


Figure 5: (A) Architecture of ANN of 2D traffic noise prediction (8-18-1), (B) architecture of ANN of 3D traffic noise prediction (22-11-1). 2D, two-dimensional; 3D, three-dimensional; ANN, artificial neural network.

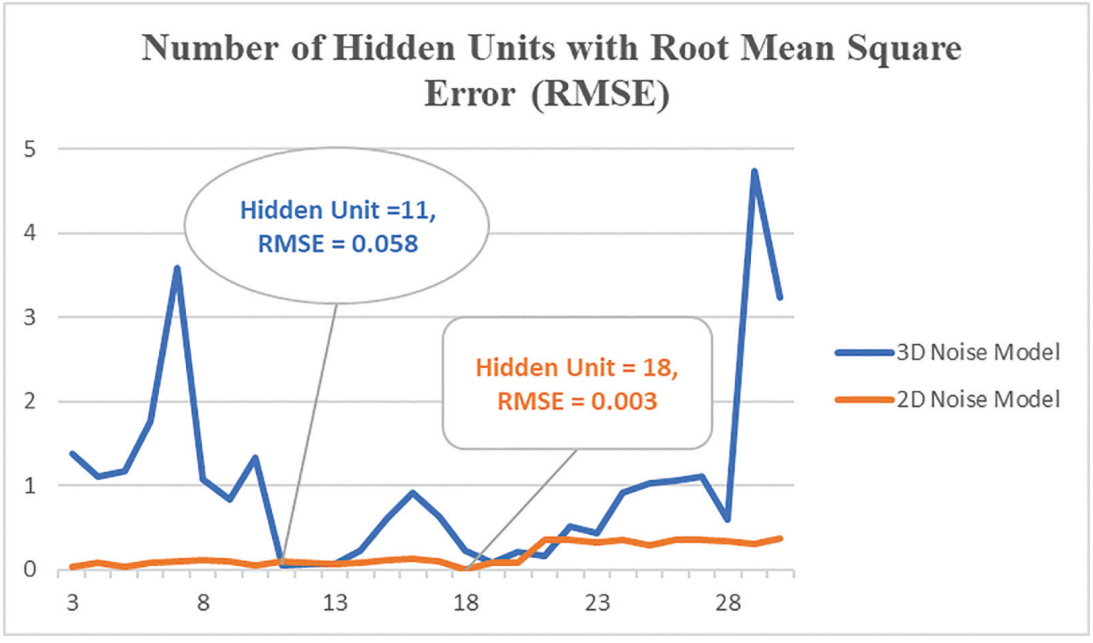


Figure 6: Number of hidden units with RMSE for 2D and 3D noise model prediction. 2D, two-dimensional; 3D, three-dimensional; RMSE, root mean square error.

ANN of hyperparameters model was used to predict traffic noise along with a search space for fine-tuning (Table 3). The ANN training model achieved an RMSE of 0.003, correlation (R), and correlation coefficient (R^2) of 1.00. The ANN test model recorded R^2 for traffic noise predictions of the RMSE of 7.14, 0.87, and 0.75 for this study area, respectively. The result of 3D noise prediction from 22 input parameters and 11 hidden layers was found to be the best for validation. The best-trained network and best hidden and issued activations were the RBFT algorithm and logistics, respectively. Also, the optimal gradient pulse and learning rate is 0.3. This network of 3D noise completeness models achieved a RMSE of 0.058 and a correlation (R) and correlation coefficient (R^2) of 1.00, whereas the test model had RMSE, R, and R^2 recorded for noise prediction.

b. Sensitivity analysis

ANN proposed model of 2D and 3D traffic noise prediction affected by several parameters which were used in this research, such as hidden number units' layer, learning rate, gradient, and activation functions for hidden and output layers. Figure 6 shows the number of hidden units with RMSE for 2D and 3D traffic noise prediction. The figure shows that the best hidden number units is 18 with RMSE = 0.003 for the best 2D noise model. The best hidden unit of 11 with RMSE (0.058) for 3D noise model was achieved. This figure shows that RMSE is increasing gradually after hidden units of 18 with an increase in hidden number units in 2D noise model, while the RMSE in 3D model was higher when the hidden units are <11 and >22.

It was observed that the training identity algorithm with an RMSE of 0.003 for the 2D noise model and RMSE of the 3D noise model was 0.058 with logistic algorithm. The training algorithms of 2D and 3D noise models were presented for BFGS and RBFT algorithms. The RMSE of the BFGS algorithm was observed to be 0.003 and 2.6287 for the 2D and 3D noise models, respectively, while the RBFT algorithm was observed to be 0.058 and 0.1746 for 2D and 3D noise models, respectively. This implies that the BFGS algorithm performs better than RBFT in the 2D noise model, whereas RBFT algorithm indicates better performance than the BFGS algorithm for the 3D noise model.

On the other hand, we found the performance of the ANN optimization model was affected by the learning rate and gradient. Figure 7 shows the learning rate and gradient impulse along with the RMSE, whereas the optimal learning rate and gradient momentum of 0.3 for 2D and 3D noise models. On the other hand, the RMSE was 0.003 and 0.058 for the 2D and 3D noise models, respectively. RMSE

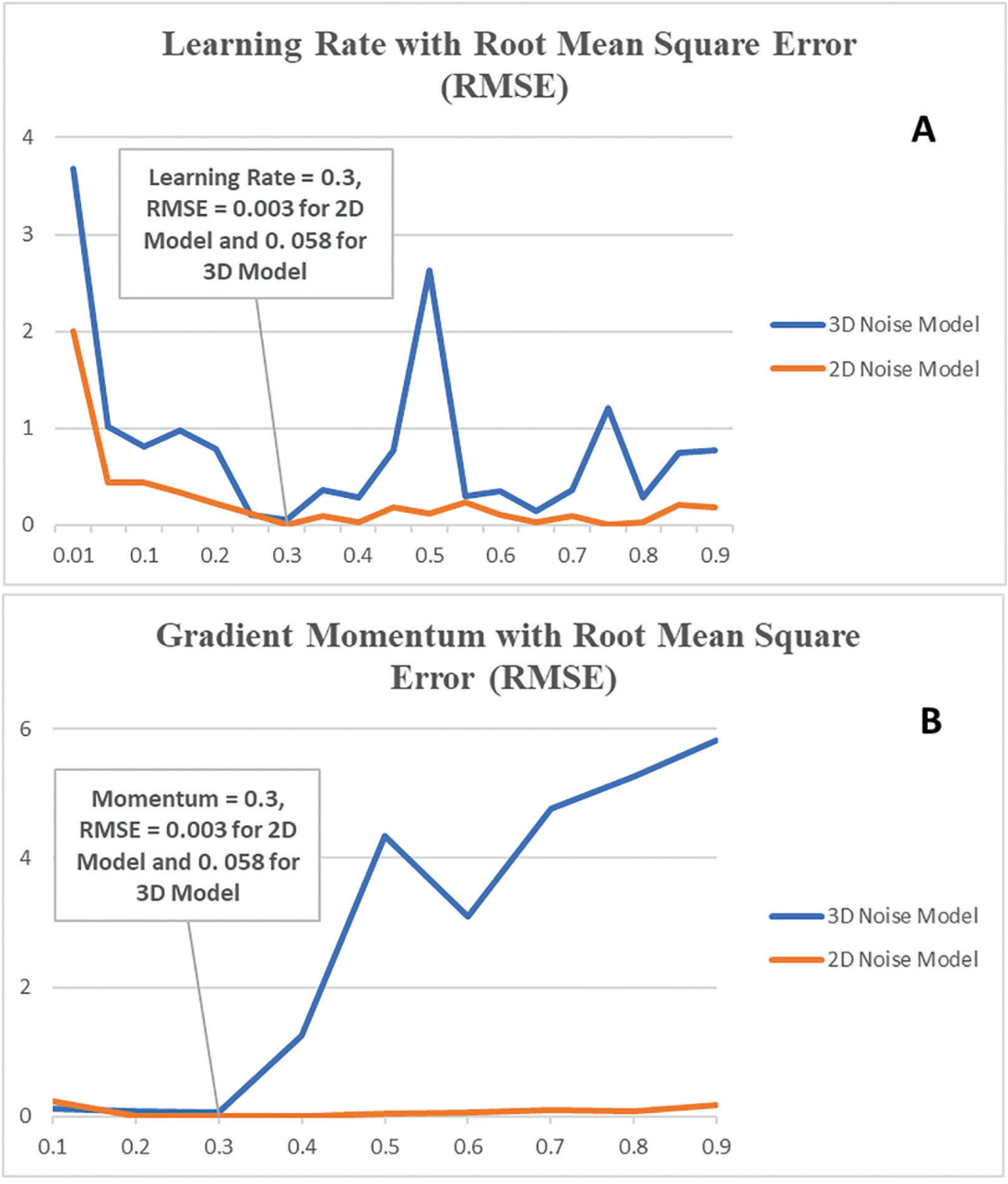


Figure 7: (A) Learning rate and (B) gradient momentum with RMSE for 2D and 3D noise model prediction. 2D, two-dimensional; 3D, three-dimensional; RMSE, root mean square error.

Table 3: Shows the hidden and output activation of the ANN model

Model	Hyperparameter	Identity	Logistic	Tanh	Exponential	Gaussian
2D Noise Model	Hidden and output activation	0.003	0.0248	0.1892	2.0043	0.2373
3D Noise Model		0.0805	0.058	0.3584	1.2066	0.1166

2D, two-dimensional; 3D, three-dimensional; ANN, artificial neural network.

decreased significantly at learning rates between 0.01 and 0.5. The RMSE gradually decreased with increasing gradient pulses and learning rate. However, gradient pulses are important if you need to avoid sticking local minima. In general, large momentum values result in faster convergence, but small values do not reliably avoid local minima that slow down the training of the system.

c. Comparison between ANN and the other models

The selected model (ANN) was compared with other models such as RF and SVM. As shown in Table 4, ANN performs better than other models, which can be seen in the R, R^2, and RMSE values for the training and test data. Figures 8A,B,C and Figures

Table 4: Performance of models such as ANN, SVM, and RF for 2D and 3D noise models

Model	Type of model	Training (R)	Testing (R)	Training (R^2)	Testing (R^2)	Training (RMSE)	Testing (RMSE)
2D Noise Model	ANN	1.00	0.87	1.00	0.75	0.003	7.14
	SVM	0.85	0.81	0.72	0.65	3.60	10.34
	RF	0.98	0.82	0.97	0.68	1.82	9.83
3D Noise Model	ANN	1.00	0.82	1.00	0.68	0.058	4.46
	SVM	0.98	0.77	0.96	0.60	6.16	4.75
	RF	0.98	0.80	0.96	0.64	6.00	4.50

2D, two-dimensional; 3D, three-dimensional; ANN, artificial neural network; R, correlation; R^2, correlation coefficient; RF, random forest; RMSE, root mean square error; SVM, support vector machine.

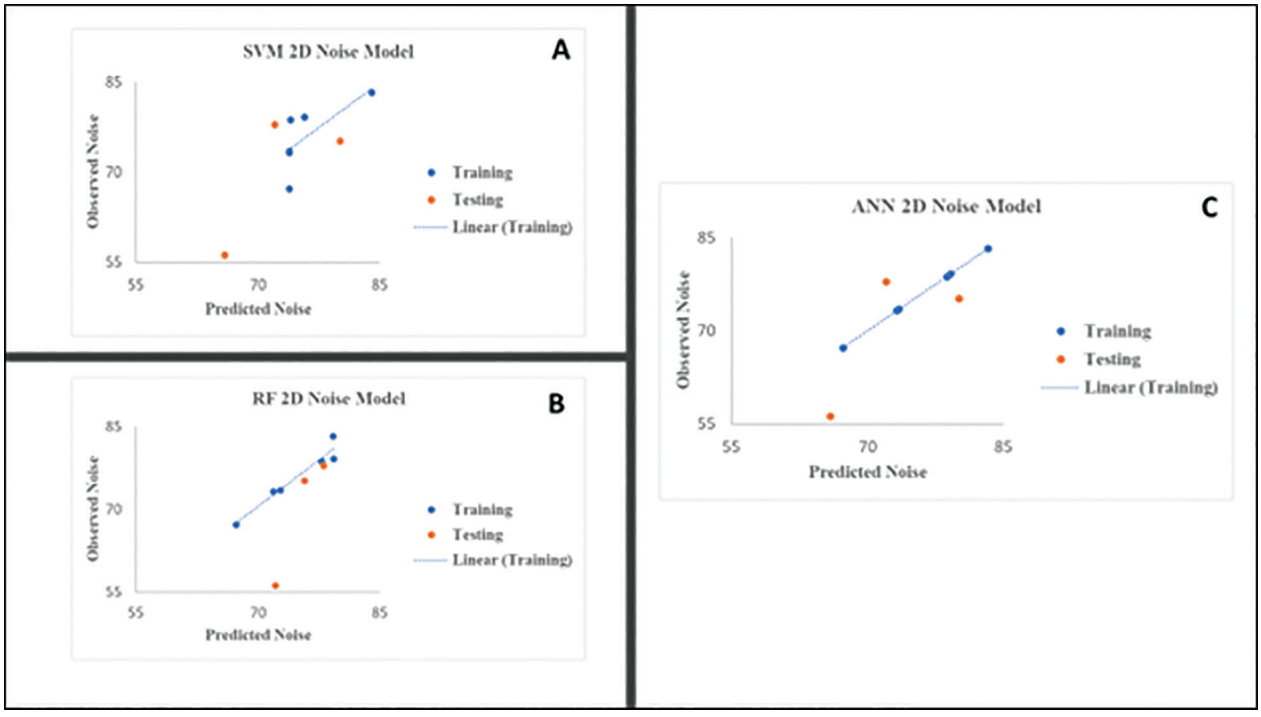


Figure 8: The correlation of training and testing noise models between observed and predicted of 2D traffic noise for (A) SVM, (B) RF, and (C) ANN models. 2D, two-dimensional; ANN, artificial neural network; RF, random forest; SVM, support vector machine.

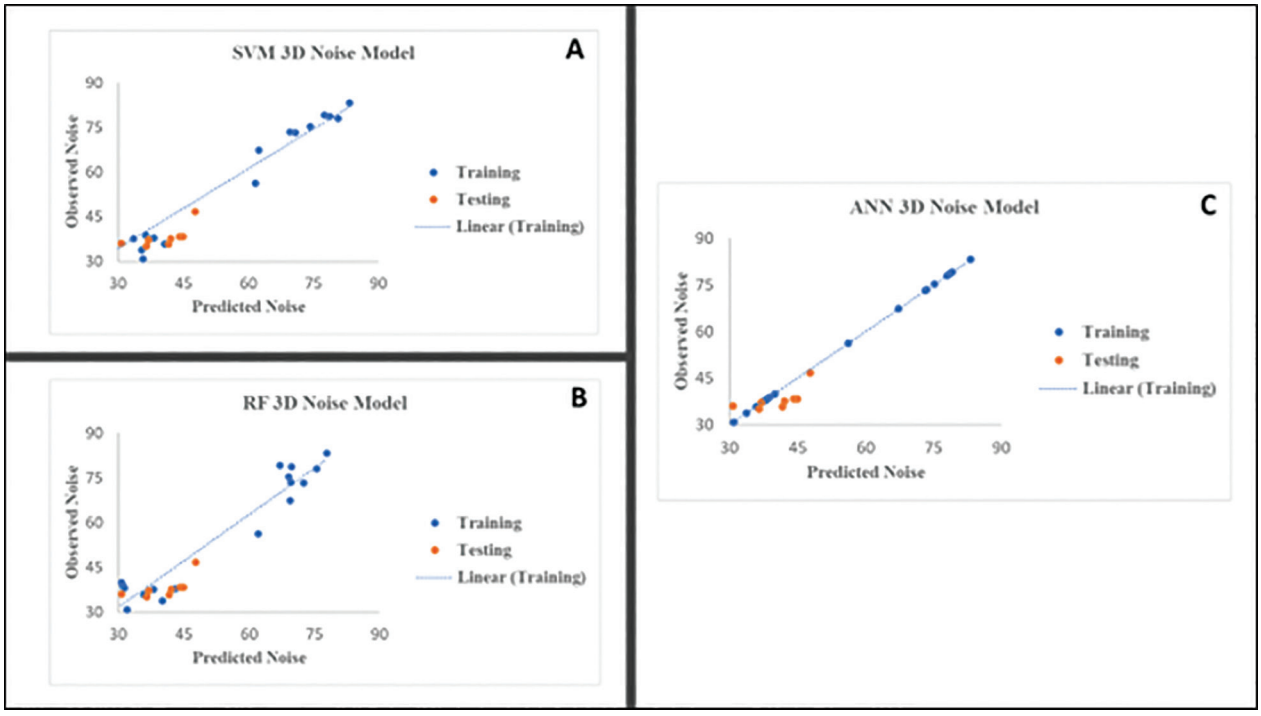


Figure 9: The correlation of training and testing noise models between observed and predicted of 3D traffic noise for (A) SVM, (B), RF, and (C) ANN models. 3D, three-dimensional; ANN, artificial neural network; RF, random forest; SVM, support vector machine.

9A,B,C show the correlation of training and testing noise models between observed and predicted of 2D (Figure 8) and 3D (Figure 9) traffic noise for ANN, RF, and SVM models.

Statistically, in the ANN model for 2D noise model, the correlation (R) and the correlation coefficient (R^2) of 1.00 were achieved and the RMSE of 0.003 was observed for training. For testing, R, R^2, and RMSE were 0.87, 0.75, and 7.14, respectively. The SVM model indicated the lowest values with R (0.85), R^2 (0.72), and RMSE (3.6) for training the model, while in testing the model, R (0.81), R^2 (0.65), and RMSE (10.34) were recorded. Lastly, in the RF model, R (0.98), R^2 (0.97), and RMSE (1.82) were recorded for training and R (0.82), R^2 (0.68), and RMSE (9.83) were for training and testing model, respectively.

For the 3D noise model, the correlation (R) and the correlation coefficient (R^2) of 1.00 were achieved, and the RMSE (0.058) was recorded for training. Whereas for the testing, R, R^2, and RMSE were 0.82, 0.68, and 4.46, respectively, for ANN model. Also, the lower model was observed to be the SVM model which was achieved at R (0.98), R^2 (0.96), and RMSE (6.16) for training model, while for the testing model, R (0.77), R^2 (0.60), and RMSE (4.75) were achieved. Lastly, the RF model was achieved with R (0.98), R^2 (0.96), and RMSE (6.00) for training and R (0.80), R^2 (0.64), and RMSE (4.50) testing model. Therefore, from the 2D and 3D noise models analyzed, the ANN model was more accurate than RF and SVM models. The SVM indicated the lowest performance.

d. 2D and 3D prediction of traffic noise maps

A noise map of the study area was created using a noise model proposed in GIS. The output of the model is a continuous noise floor that accounts for other factors such as field conditions and topography. In this study, noise and traffic were measured at different times: morning and afternoon on weekdays. The 2D noise prediction for roads in the study area is shown in Figure 10, whereas the 3D noise prediction for buildings is shown in Figures 11A,B. The noise projections for the entire study area, this is a combination of 2D and 3D noise maps as Figure 11C. However, this section only contains maps that are recommended for planning purposes. We found this road to be characterized by heavy traffic noise during the morning and afternoon hours. The figure below

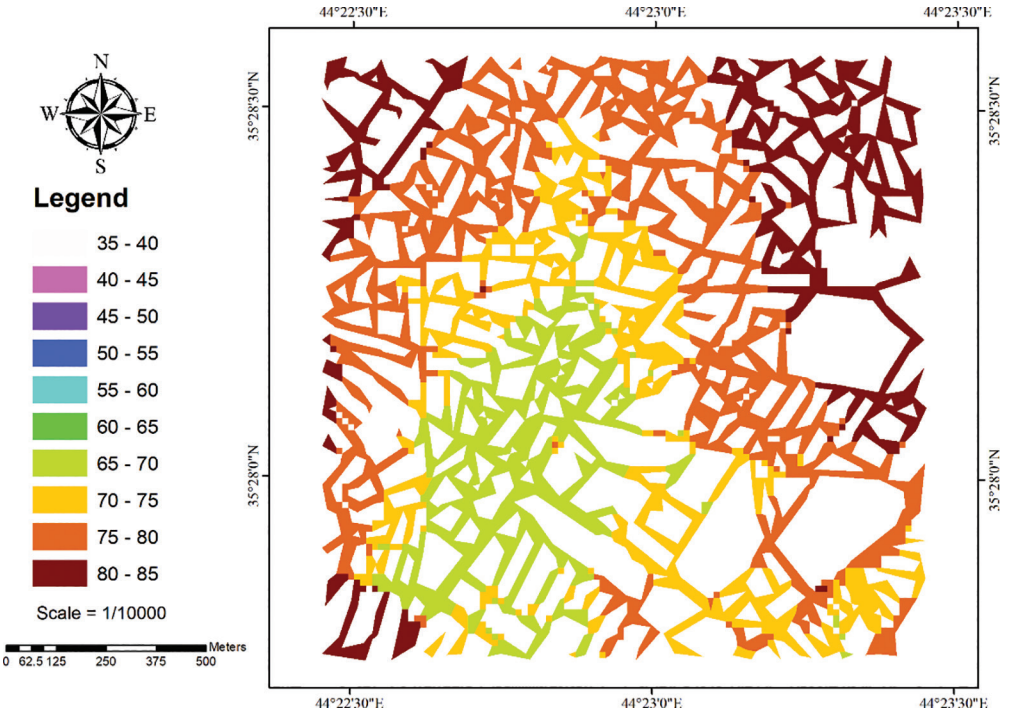


Figure 10: 2D average noise prediction map for roads in the study area from 2D ANN noise model. 2D, two-dimensional; ANN, artificial neural network.

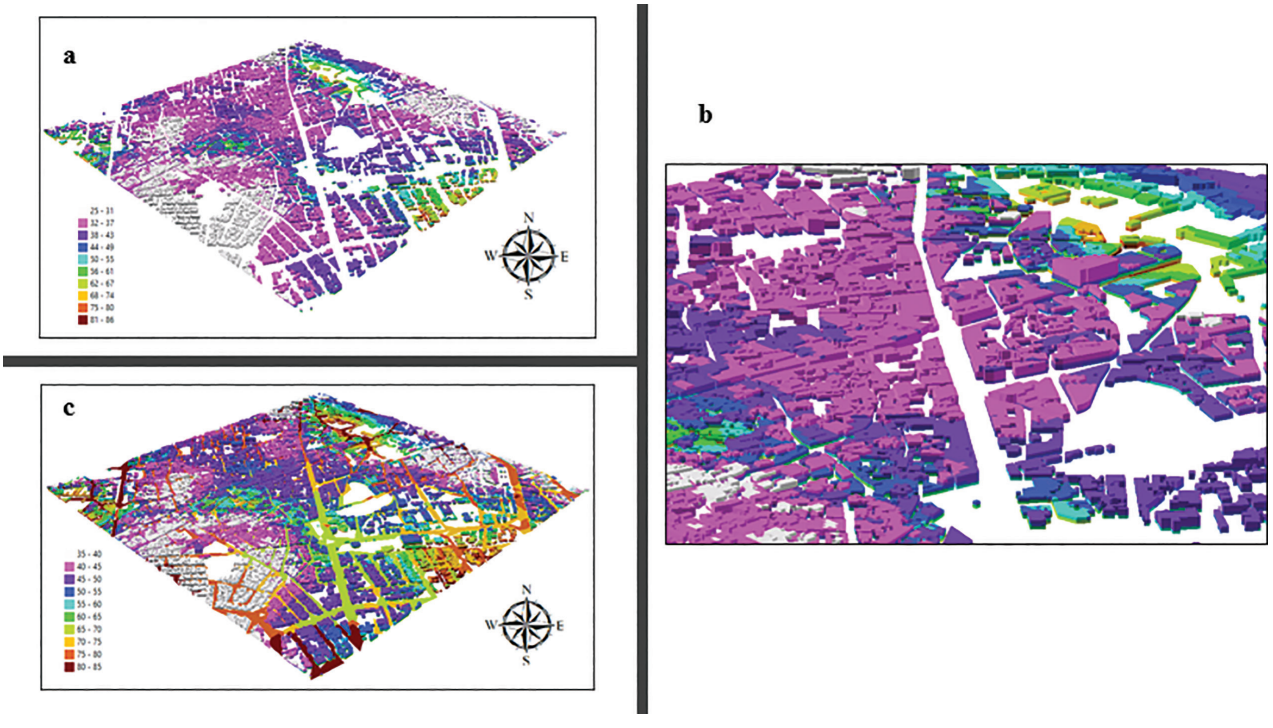


Figure 11: (A) 3D average noise prediction map for building in the study area from the 3D noise model, (B) average noise prediction map for building in the study area from the 3D noise model for part of the study area, (C) average noise prediction map for roads and building at the study area through combined 2D and 3D model maps. 2D, two-dimensional; 3D, three-dimensional.

shows the proposed noise distribution map (mean traffic noise level) for the study area on weekday mornings and afternoons.

VII. Conclusions

Vehicular traffic noise is one of the major sources of environmental pollution in urban areas, where road networks and traffic flow are present. Traffic noise prediction models and spatial models are used to assess the impacts of vehicular emissions on human health and the environment. In this study, noise impact and improved visualization of the noise impact are proposed using 2D and 3D GIS functionalities. This approach is aimed at improving the accuracy of noise impact assessment studies using fewer noise samples. The two models such as 2D noise model for roads and 3D noise model for buildings are developed and combined to produce the final 3D noise map for the capital of the study area, which is considered the novelty of this research. The proposed 2D model noise prediction achieved 0.003 for RMSE, 1.00 for correlation (R), and correlation coefficient (R^2) of 1. For the testing model, 7.14, 0.87, and 0.75 were recorded for RMSE, R, and R^2 of the traffic noise prediction, respectively. The proposed 3D noise prediction model shows 0.058 for RMSE and 1.00 for correlation (R), correlation coefficient (R^2). For the testing model, 4.46, 0.82, and 0.68 were recorded for RMSE, R, and R^2 of the traffic noise prediction, respectively. The result shows that the best architecture in the 2D ANN noise prediction model was achieved by a network of 8 input parameters, 18 hidden layers, BFGS algorithm of trained network, identity algorithm of hidden and output activation, and 0.3 of gradient momentum and learning rate. While the best architecture in the 3D ANN noise prediction model was achieved by a network of 22 input parameters, 11 hidden layers, RBFT algorithm of trained of network, logistic algorithm of hidden and output activation, and 0.3 of gradient momentum and learning rate. Moreover, it was observed that the best model is ANN, and RF is better than SVM. This was evident by the result that RF is less than RMSE of SVM, whereas RMSE of RF model was (1.82, 6.00) and (9.83, 4.50) for training and testing 2D and 3D model, respectively, while RMSE of SVM model was (3.60, 6.16) and (10.34, 4.75) for training and testing 2D and 3D model, respectively. The GIS modeling was applied to improve visualization of 2D and 3D noise maps and these maps were the average traffic noise level of the study area for weekdays in the morning and afternoon.

Author Contributions

Conceptualization, B.P.; resources, B.P.; methodology, B.P. and A.A.A.A.; software, B.P.; validation, A.A.A.A., B.P., S.G.; formal analysis, A.A.A.A.; investigation, A.A.A.A. and B.P.; data curation, A.A.A.A.; writing, A.A.A.A.; writing—review and editing, B.P., S.G., S.M., and A.A.; visualization, B.P., S.G., S.M., and A.A.; supervision, B.P.; project administration, B.P.; funding acquisition, B.P. and A.A. All authors have read and agreed to the published version of the manuscript.

Declaration of competing interest

The authors declare that they have no known competing financial interests or personal relationships that could have appeared to influence the work reported in this article.

Funding

This work was supported by the Australian Government Research Training Program, the Centre for Advanced Modelling and Geospatial Information Systems (CAMGIS), Faculty of Engineering and Information Technology, University of Technology Sydney (UTS), Australia, in part by the Researchers Supporting Project, King Saud University, Riyadh, Saudi Arabia, under Project RSP2024 R14.

Data Availability Statement

The data used in this study are available from the corresponding author.

References

[1] Vigar, G. (2013). The politics of mobility: Transport planning, the environment and public policy. Routledge.

[2] Pink, S., Lacey, J., Harvey, L., Sumartojo, S., Duque, M., & Moore, S. (2019). Recycling traffic noise: transforming sonic automobilities for revalue and well-being. Mobilities, 14(2), 233-249.

[3] Morley, D. W., De Hoogh, K., Fecht, D., Fabbri, F., Bell, M., Goodman, P. S., Elliott, P., Hodgson, S., Hansell, A. L. & Gulliver, J. (2015). International scale implementation of the CNOSSOS-EU road traffic noise prediction model for epidemiological studies. Environmental pollution, 206, 332-341.

[4] Babisch, W. (2008). Road traffic noise and cardiovascular risk. Noise and Health, 10(38), 27.

[5] Cervero, R. (1998). The transit metropolis: a global inquiry. Island press.

[6] Dahl, R. (2005). Heavy traffic ahead: car culture accelerates.

[7] Johansson, O., Pearce, D., & Maddison, D. (2014). Blueprint 5: True costs of road transport. Routledge.

[8] Hurtley, C. (Ed.). (2009). Night noise guidelines for Europe. WHO Regional Office Europe.

[9] Ahmed, A. A., & Pradhan, B. (2019). Vehicular traffic noise prediction and propagation modelling using neural networks and geospatial information system. Environmental monitoring and assessment, 191(3), 190.

[10] Morley, D. W., & Gulliver, J. (2016). Methods to improve traffic flow and noise exposure estimation on minor roads. Environmental pollution, 216, 746-754.

[11] Steele, C. (2001). A critical review of some traffic noise prediction models. Applied acoustics, 62(3), 271-287.

[12] Suárez, E., & Barros, J. L. (2014). Traffic noise mapping of the city of Santiago de Chile. Science of the total environment, 466, 539-546.

[13] Torija, A. J., & Ruiz, D. P. (2012). Using recorded sound spectra profile as input data for real-time short-term urban road-traffic-flow estimation. Science of the total environment, 435, 270-279.

[14] Tang, U. W., & Wang, Z. S. (2007). Influences of urban forms on traffic-induced noise and air pollution: Results from a modelling system. Environmental Modelling & Software, 22(12), 1750-1764.

[15] Tomczak, M. (1998). Spatial interpolation and its uncertainty using automated anisotropic inverse distance weighting (IDW)-cross-validation/jackknife approach. Journal of Geographic Information and Decision Analysis, 2(2), 18-30.

[16] Tomić, J., Bogojević, N., Pljakić, M., & Šumarac-Pavlović, D. (2016). Assessment of traffic noise levels in urban areas using different soft computing techniques. The Journal of the Acoustical Society of America, 140(4), EL340–EL345.

[17] Andersen, Z. J., Jørgensen, J. T., Elsborg, L., Lophaven, S. N., Backalarz, C., Laursen, J. E., … & Lynge, E. (2018). Long-term exposure to road traffic noise and incidence of breast cancer: a cohort study. Breast Cancer Research, 20(1), 119.

[18] Halim, H., Abdullah, R., Nor, M. M., Aziz, H. A., & Rahman, N. A. (2017). Comparison between measured traffic noise in Klang Valley, Malaysia and existing prediction models. Engineering Heritage Journal, 1(2), 10-14.

[19] Yamamoto, K., Yoshihisa, K., Miyake, T., Tajika, T., & Tachibana, H. (2018). Road traffic noise prediction model "ASJ RTN-Model 2003" proposed by the Acoustical Society of Japan-Part 3: Calculation model of sound propagation. In the Proceedings of the 18th International Congress on Acoustics (ICA) (pp. 4-9).

[20] Gulliver, J., Morley, D., Vienneau, D., Fabbri, F., Bell, M., Goodman, P., … & Fecht, D. (2015). Development of an open-source road traffic noise model for exposure assessment. Environmental Modelling & Software, 74, 183-193.

[21] Sakamoto, S. (2015). Road traffic noise prediction model ``ASJ RTN-Model 2013'': Report of the Research Committee on Road Traffic Noise. Acoustical Science and Technology, 36(2), 49-108.

[22] Steele, C. (2001). A critical review of some traffic noise prediction models. Applied acoustics, 62(3), 271-287.

[23] Liu, B., Li, K., Huang, D. S., & Chou, K. C. (2018). iEnhancer-EL: identifying enhancers and their strength with ensemble learning approach. Bioinformatics, 34(22), 3835-3842.

[24] Zhang, C., & Ma, Y. (Eds.). (2012). Ensemble machine learning: methods and applications. Springer Science & Business Media.

[25] Polikar, R. (2012). Ensemble learning. In Ensemble machine learning (pp. 1-34). Springer, Boston, MA.

[26] Kulkarni, S., & Kelkar, V. (2014, April). Classification of multispectral satellite images using ensemble techniques of bagging, boosting and adaboost. In 2014 International Conference on Circuits, Systems, Communication and Information Technology Applications (CSCITA) (pp. 253-258). IEEE.

[27] Sengur, A. (2012). Support vector machine ensembles for intelligent diagnosis of valvular heart disease. Journal of medical systems, 36(4), 2649-2655.

[28] Ghimire, B., Rogan, J., Galiano, V. R., Panday, P., & Neeti, N. (2012). An evaluation of bagging, boosting, and random forests for land-cover classification in Cape Cod, Massachusetts, USA. GIScience & Remote Sensing, 49(5), 623-643.

[29] Deng, Y., Cheng, J. C., & Anumba, C. (2016). A framework for 3D traffic noise mapping using data from BIM and GIS integration. Structure and Infrastructure Engineering, 12(10), 1267-1280.

[30] Stoter, J., De Kluijver, H., & Kurakula, V. (2008). 3D noise mapping in urban areas. International Journal of Geographical Information Science, 22(8), 907-924.

[31] Law, C. W., Lee, C. K., Lui, A. S. W., Yeung, M. K. L., & Lam, K. C. (2011). Advancement of three-dimensional noise mapping in Hong Kong. Applied Acoustics, 72(8), 534-543.

[32] Alam, P., Ahmad, K., Afsar, S. S., & Akhtar, N. (2020). 3D noise mapping for preselected locations of urban area with and without noise barriers: A case study of Delhi, India. Noise Mapping, 7(1), 74-83.

[33] Zhao, W. J., Liu, E. X., Poh, H. J., Wang, B., Gao, S. P., Png, C. E., Li KW & Chong, S. H. (2017). 3D traffic noise mapping using unstructured surface mesh representation of buildings and roads. Applied Acoustics, 127, 297-304.

[34] Kurakula, V. K., & Kuffer, M. (2008). 3D noise modeling for urban environmental planning and management. na.

[35] Alam, P., Ahmad, K., Afsar, S. S., & Akhtar, N. (2020). Noise monitoring, mapping, and modelling studies–a review. Journal of Ecological Engineering, 21(4).

[36] Babisch, W., Beule, B., Schust, M., Kersten, N., & Ising, H. (2005). Traffic noise and risk of myocardial infarction. Epidemiology, 33-40.

[37] Bluhm, G. L., Berglind, N., Nordling, E., & Rosenlund, M. (2007). Road traffic noise and hypertension. Occupational and environmental medicine, 64(2), 122-126.

[38] Pradhan, B., Azeez, O. S., Jena, R., Jung, H. S., & Ahmed, A. A. (2019). Traffic emission modelling using LiDAR derived parameters and integrated geospatial model. Korean Journal of Remote Sensing.

[39] Ahmed, A. A., Pradhan, B., Chakraborty, S., & Alamri, A. (2021). Developing vehicular traffic noise prediction model through ensemble machine learning algorithms with GIS. Arabian Journal of Geosciences, 14(16), 1-14.

[40] Ahmed, A. A., Pradhan, B., Chakraborty, S., Alamri, A., & Lee, C. W. (2021). An Optimized Deep Neural Network Approach for Vehicular Traffic Noise Trend Modeling. IEEE Access, 9, 107375-107386.

[41] Seong, J. C., Park, T. H., Ko, J. H., Chang, S. I., Kim, M., Holt, J. B., & Mehdi, M. R. (2011). Modeling of road traffic noise and estimated human exposure in Fulton County, Georgia, USA. Environment international, 37(8), 1336-1341.

[42] Diallo, T. M., Collignan, B., & Allard, F. (2015). 2D Semi-empirical models for predicting the entry of soil gas pollutants into buildings. Building and Environment, 85, 1-16.

[43] dos Santos, D. R., Cambier, P., Mallmann, F. J. K., Labanowski, J., Lamy, I., Tessier, D., & van Oort, F. (2013). Prospective modeling with Hydrus-2D of 50 years Zn and Pb movements in low and moderately metal-contaminated agricultural soils. Journal of contaminant hydrology, 145, 54-66.

[44] Duan, Q., Lee, J., Liu, Y., Chen, H., & Hu, H. (2016). Distribution of heavy metal pollution in surface soil samples in China: a graphical review. Bulletin of environmental contamination and toxicology, 97(3), 303-309.

[45] Butler, D. (2004). Noise management: Sound and vision. Nature, 427(6974), 480-482.

[46] Law, C. W., Lee, C. K., Lui, A. S. W., Yeung, M. K. L., & Lam, K. C. (2011). Advancement of three-dimensional noise mapping in Hong Kong. Applied Acoustics, 72(8), 534-543.

[47] ISO, I. (1996). 9613-2-Acoustics. Attenuation of sound during propagation outdoors. Part, 2.

[48] DoT, U. K. (1988). Calculation of road traffic noise.

[49] Kurakula, V., Skidmore, A., Kluijver, H., Stoter, J., Dabrowska Zielinska, K., & Kuffer, M. (2007, March). A GIS based approach for 3D noise modelling using 3D city models. Enschede, The Netherlands: ITC.

[50] May, R., Dandy, G., & Maier, H. (2011). Review of input variable selection methods for artificial neural networks. Artificial neural networks-methodological advances and biomedical applications, 10, 16004.

[51] Iniesta, R., Stahl, D., & McGuffin, P. (2016). Machine learning, statistical learning and the future of biological research in psychiatry. Psychological medicine, 46(12), 2455-2465.

[52] Goyal, M. K., Bharti, B., Quilty, J., Adamowski, J., & Pandey, A. (2014). Modeling of daily pan evaporation in sub-tropical climates using ANN, LS-SVR, Fuzzy Logic, and ANFIS. Expert systems with applications, 41(11), 5267-5276.

[53] Kang, J., Schwartz, R., Flickinger, J., & Beriwal, S. (2015). Machine learning approaches for predicting radiation therapy outcomes: a clinician's perspective. International Journal of Radiation Oncology* Biology* Physics, 93(5), 1127-1135.

[54] Akhter, M. N., Mekhilef, S., Mokhlis, H., & Mohamed Shah, N. (2019). Review on forecasting of photovoltaic power generation based on machine learning and metaheuristic techniques. IET Renewable Power Generation, 13(7), 1009-1023.

[55] Bishop, C. M. (1995). Neural networks for pattern recognition. Oxford university press.

[56] Hill, D. J., & Minsker, B. S. (2010). Anomaly detection in streaming environmental sensor data: A data-driven modeling approach. Environmental Modelling & Software, 25(9), 1014-1022.

[57] Baczynski, D., & Parol, M. (2004). Influence of artificial neural network structure on quality of

short-term electric energy consumption forecast. IEE Proceedings-Generation, Transmission and Distribution, 151(2), 241-245.

[58] Yang, G. Y. (1996). Geological mapping from multi-source data using neural networks.

[59] Caruana, R., & Niculescu-Mizil, A. (2006, June). An empirical comparison of supervised learning algorithms. In Proceedings of the 23rd international conference on Machine learning (pp. 161-168).

[60] Xu, B., Ye, Y., & Nie, L. (2012, June). An improved random forest classifier for image classification. In 2012 IEEE International Conference on Information and Automation (pp. 795-800). IEEE.

[61] Kulkarni, A. D., & Lowe, B. (2016). Random forest algorithm for land cover classification.

[62] Dubath, P., Rimoldini, L., Süveges, M., Blomme, J., López, M., Sarro, L. M., Sarro LM, De Ridder J, Cuypers J, Guy L, Lecoeur I, Nienartowicz K & Eyer, L. (2011). Random forest automated supervised classification of Hipparcos periodic variable stars. Monthly Notices of the Royal Astronomical Society, 414(3), 2602-2617.

[63] VijiyaKumar, K., Lavanya, B., Nirmala, I., & Caroline, S. S. (2019, March). Random forest algorithm for the prediction of diabetes. In 2019 IEEE International Conference on System, Computation, Automation and Networking (ICSCAN) (pp. 1-5). IEEE.

[64] Ranković, V., Grujović, N., Divac, D., & Milivojević, N. (2014). Development of support vector regression identification model for prediction of dam structural behaviour. Structural Safety, 48, 33-39.

[65] Hong, X., Mitchell, R. J., Chen, S., Harris, C. J., Li, K., & Irwin, G. W. (2008). Model selection approaches for non-linear system identification: a review. International journal of systems science, 39(10), 925-946.

[66] Adulaimi, A. A. A., Pradhan, B., Chakraborty, S., & Alamri, A. (2021). Traffic Noise Modelling Using Land Use Regression Model Based on Machine Learning, Statistical Regression and GIS. Energies, 14(16), 5095.